mathematics

MDPI

Article

A Spectral Approach to Variable-Order Fractional Differential Equations: Improved Operational Matrices for Fractional Jacobi Functions

Hany M. Ahmed [1], Mohammad Izadi [2] and Carlo Cattani [3,*]

[1] Department of Mathematics, Faculty of Technology and Education, Helwan University, Cairo 11281, Egypt; hanyahmed@techedu.helwan.edu.eg
[2] Department of Applied Mathematics, Faculty of Mathematics and Computer, Shahid Bahonar University of Kerman, Kerman 76169-14111, Iran; izadi@uk.ac.ir
[3] Engineering School (DEIM), University of Tuscia, 01100 Viterbo, Italy
* Correspondence: cattani@unitus.it

Abstract

The current paper presents a novel numerical technique to handle variable-order multiterm fractional differential equations (VO-MTFDEs) supplemented with initial conditions (ICs) by introducing generalized fractional Jacobi functions (GFJFs). These GFJFs satisfy the associated ICs. A crucial part of this approach is using the spectral collocation method (SCM) and building operational matrices (OMs) for both integer-order and variable-order fractional derivatives in the context of GFJFs. These lead to efficient and accurate computations. The suggested algorithm's convergence and error analysis are proved. The feasibility of the suggested procedure is confirmed via five numerical test examples.

Keywords: collocation method; Liouville–Caputo derivative; variable-order fractional differential equations; fractional Jacobi functions; Jacobi polynomials; initial value problems; generalized hypergeometric functions

MSC: 42C05; 65L60; 34B05



Academic Editor: Sotiris K. Ntouyas

Received: 12 July 2025
Revised: 2 August 2025
Accepted: 6 August 2025
Published: 8 August 2025

Citation: Ahmed, H.M.; Izadi, M.; Cattani, C. A Spectral Approach to Variable-Order Fractional Differential Equations: Improved Operational Matrices for Fractional Jacobi Functions. *Mathematics* **2025**, *13*, 2544. https://doi.org/10.3390/math13162544

Copyright: © 2025 by the authors. Licensee MDPI, Basel, Switzerland. This article is an open access article distributed under the terms and conditions of the Creative Commons Attribution (CC BY) license (https://creativecommons.org/licenses/by/4.0/).

1. Introduction

The past few decades have witnessed growing interest in fractional calculus (FC) among researchers from diverse fields. This surge in attention is largely attributed to the fact that fractional operators offer a more comprehensive approach to characterizing dynamic systems than traditional integer-order methods [1–4]. A recent development in FC related to the extension of variable-order fractional differential equations (VOFDs). The characteristics of VOFD operators are studied in [5–7]. VOFDs have been extensively utilized in control, physics, mechanics, and signal processing (see, for instance, [8–11]). Beyond system dynamics, fractional calculus has found application in materials science for describing complex microstructural properties [12]. The Riesz–Caputo formulation with space-dependent fractional order has shown particular promise in continuum elasticity problems [13]. Additionally, they were employed to represent the microscopic structure of materials. The Riesz–Caputo fractional derivative of spatially dependent order was utilized in continuum elasticity, as seen in [13].

Significant advances in numerical analysis have yielded multiple robust methods for approximating solutions to this category of equations. In prior studies, scholars have

utilized several methodologies to formulate numerical solutions (NUMSs) for fractional differential equations (FDEs) through spectral methods employing various polynomial systems, including both orthogonal and non-orthogonal families (refer to, for example, [14–31]), whereas Bernstein polynomials were utilized in [32,33]. A numerical technique utilizing Fourier analysis was proposed in [34]. In [35], the suggested systems were examined based on finite difference approximations. In [36], a numerical method is introduced, based on Bernoulli polynomials, for solving VO-MTFDEs.

Orthogonal JPs [37–47] have multiple beneficial characteristics that make them exceptionally useful in the numerical resolution of diverse forms of differential equations (DEs), especially using spectral approaches. Jacobi polynomials offer three principal advantages: a built-in orthogonal structure, rapid spectral convergence, and shape parameters that provide control over approximation properties.

Orthogonal functions (OFs) have garnered significant interest in addressing FDEs [48–50]. The primary attribute of this strategy is its ability to reduce these fractional model problems to the handling of an algebraic system of equations, so significantly simplifying the problem. Reference [48] presented a fractional generalization of Legendre orthogonal functions, constructed from standard Legendre polynomials, for obtaining spectrally accurate solutions to FDEs in bounded domains. Building on this work, Ref. [51] introduced a bivariate extension of these fractional-order basis functions and established their associated operational matrices for derivative and integral operators, facilitating the numerical treatment of 2D fractional problems. Notably, Izadi and Cattani [52] developed generalized Bessel polynomials for solving multi-order FDEs, demonstrating their effectiveness through rigorous convergence analysis. Furthermore, for solving FDEs on semi-infinite intervals, the authors in [53] developed fractional integral operators based on generalized Laguerre operational matrices. Separately, reference [54] presented an eigenvalue–eigenvector approach for handling systems of FDEs with uncertainty.

This study extends the application of novel orthogonal functions derived from Jacobi polynomials to solve variable-order FDEs. We employ the following generalized fractional Jacobi functions that inherently satisfy the prescribed initial conditions to develop a spectral collocation method for VO-MTFDEs:

$$ {}_0^{LC}\mathbb{D}_\tau^{\nu(\tau)}\chi(\tau) = F\Big(\tau, \chi(\tau), {}_0^{LC}\mathbb{D}_\tau^{\nu_1(\tau)}\chi(\tau), {}_0^{LC}\mathbb{D}_\tau^{\nu_2(\tau)}\chi(\tau), \ldots, {}_0^{LC}\mathbb{D}_\tau^{\nu_m(\tau)}\chi(\tau)\Big), \tag{1} $$

for $\tau \in (0, \ell)$ and supplemented with the subsequent ICs, written as follows:

$$ \chi^{(s)}(0) = \omega_s, \qquad s = 0, 1, \ldots, n-1, \tag{2} $$

where $0 < \nu_1(\tau) < \nu_2(\tau) < \cdots < \nu_m(\tau) < \nu(\tau) \leq n$ holds, n is the smallest positive integer number such that for all $\tau \in [0, \ell]$, and ${}_0^{LC}\mathbb{D}_\tau^{\nu(\tau)}\chi(\tau)$ and ${}_0^{LC}\mathbb{D}_\tau^{\nu_i(\tau)}\chi(\tau)$ stand for the VOFDs defined in the Liouville–Caputo sense for $i = 1, 2, \ldots, m$. The mathematical frameworks represented by Equations (1) and (2) possess significant practical utility across various domains. Notable applications include signal processing and noise reduction [55,56], geographical information processing [57], and handwritten signature analysis [58], underscoring their versatility in solving applied problems.

We have devised an innovative approach to address (1) and (2) by formulating new Galerkin operational matrices (OMs) for ordinary derivatives ODs and VOFDs for the basis vector of GFJFs. Based on what we know, the literature has never before seen this strategy for addressing VO-MTFDEs, utilizing the Liouville–Caputo FDs of the suggested basis vector, as been presented. This innovative technique facilitates the successful healing and acquisition of NUMSs for this category of FDEs.

This article is organized as follows: In Section 2, we present an overview of the core concepts and basic of VOFD. Section 3 highlights specific properties of the shifted JPs and

fractional Jacobi functions (FJFs). Section 4 concentrates on the creation of innovative OMs for ODs and VOFDs of GFJFs. In Section 5, we investigate the use of newly constructed OMs alongside the SCM as an approximate method to address (1) and (2). The assessment of the error estimate for the NUMSs derived from this novel method is detailed in Section 6. Numerical simulations of test cases are conducted, and comparisons with existing methodologies from the literature demonstrate the efficacy of the proposed approach. In the final Section 8, we encapsulate the primary findings and derive conclusions from the current research investigation.

2. Core Definition of Liouville–Caputo VOFDs

The current section describes the key mathematical principles of fractional calculus, which are essential for implementing our proposed solution.

Definition 1 ([4,17,33,59]). *The Liouville–Caputo VOFDs for $\Theta(\tau)$ is expressed as follows:*

$$ {}_{0}^{LC}\mathbb{D}_{\tau}^{\nu(\tau)}\,\Theta(\tau) := \frac{1}{\Gamma(n-\nu(\tau))}\int_{0}^{\tau}\frac{\Theta^{(n)}(\sigma)}{(\tau-\sigma)^{1-n+\nu(\tau)}}\,d\sigma, \quad \tau>0, \quad n-1<\nu(\tau)\le n. \tag{3}$$

When $\nu(\tau)=\varsigma_1$, in Definition 1 we get the Liouville–Caputo FD of order ς_1. The core properties of the Liouville–Caputo VOFD operator are summarized as follows:

$$ {}_{0}^{LC}\mathbb{D}_{\tau}^{\nu(\tau)}(\lambda_1\Theta_1(\tau)+\lambda_2\Theta_2(\tau)) = \lambda_1\,{}_{0}^{LC}\mathbb{D}_{\tau}^{\nu(\tau)}\Theta_1(\tau)+\lambda_2\,{}_{0}^{LC}\mathbb{D}_{\tau}^{\nu(\tau)}\Theta_2(\tau), \tag{4a}$$

$$ {}_{0}^{LC}\mathbb{D}_{\tau}^{\nu(\tau)}\Theta(\tau) = \frac{d^n\Theta(\tau)}{d\,\tau^n}, \quad \nu(\tau)=n,\ n\in\mathbb{N}. \tag{4b}$$

As demonstrated in [17,33], we obtain the following:

$$ {}_{0}^{LC}\mathbb{D}_{\tau}^{\nu(\tau)}\tau^{s} = \begin{cases} 0, & s=0,\\ \dfrac{\Gamma(s+1)}{\Gamma(s+1-\nu(\tau))}\tau^{s-\nu(\tau)}, & s=1,2,\ldots,\end{cases} \tag{5a}$$

$$ {}_{0}^{LC}\mathbb{D}_{\tau}^{\nu(\tau)}(c) = 0, \qquad (c \text{ is a constant}). \tag{5b}$$

3. Shifted Jacobi Polynomials and Fractional Jacobi Functions

We first examine the fundamental properties of shifted Jacobi polynomial (JPs) systems and their fractional counterparts FJFs. Subsequently, we propose and characterize a new set of orthogonal functions (OFs), the generalized fractional Jacobi functions (GFJFs).

3.1. Analytical Framework: Shifted JP Basis Functions

For parameters $\varsigma_1,\varsigma_2>-1$, the JP family $\{\mathrm{P}_n^{(\varsigma_1,\varsigma_2)}(x)\}_{n=0}^{\infty}$ forms an orthogonal system with regard to the weight function $w^{\varsigma_1,\varsigma_2}(x)=(1-x)^{\varsigma_1}(1+x)^{\varsigma_2}$ on $[-1,1]$, as established in [60], written as follows:

$$ \int_{-1}^{1} w^{\varsigma_1,\varsigma_2}(x)\,\mathrm{P}_n^{(\varsigma_1,\varsigma_2)}(x)\,\mathrm{P}_m^{(\varsigma_1,\varsigma_2)}(x)\,dx = \begin{cases} 0, & n\neq m,\\ h_n^{(\varsigma_1,\varsigma_2)}, & n=m,\end{cases}$$

where $h_n^{(\varsigma_1,\varsigma_2)} = \dfrac{\Gamma(n+\varsigma_1+1)\,2^{\lambda}\,\Gamma(n+\varsigma_2+1)}{(2n+\lambda)\,n!\,\Gamma(n+\lambda)}$ with $\lambda=\varsigma_1+\varsigma_2+1$.

The so-called shifted JPs, $\mathrm{P}_{\ell,n}^{(\varsigma_1,\varsigma_2)}(\tau) = \mathrm{P}_n^{(\varsigma_1,\varsigma_2)}(2\tau/\ell - 1)$, obey the following orthogonality relation:

$$\int_0^\ell w_\ell^{\varsigma_1,\varsigma_2}(\tau)\, \mathrm{P}_{\ell,n}^{(\varsigma_1,\varsigma_2)}(\tau)\, \mathrm{P}_{\ell,m}^{(\varsigma_1,\varsigma_2)}(\tau)\, d\tau = \begin{cases} 0, & m \neq n, \\ \left(\frac{\ell}{2}\right)^\lambda h_n^{(\varsigma_1,\varsigma_2)}, & m = n, \end{cases}$$

where $w_\ell^{\varsigma_1,\varsigma_2}(\tau) = (\ell - \tau)^{\varsigma_1}\, \tau^{\varsigma_2}$.

The $\mathrm{P}_{\ell,n}^{(\varsigma_1,\varsigma_2)}(\tau)$ admits the following power series expansion:

$$\mathrm{P}_{\ell,i}^{(\varsigma_1,\varsigma_2)}(\tau) = \sum_{k=0}^{i} c_k^{(i)} \left(\frac{\tau}{\ell}\right)^k, \tag{6}$$

where we have defined the following:

$$c_k^{(i)} = (-1)^{i-k} \frac{\Gamma(i+\varsigma_2+1)\Gamma(i+k+\lambda)}{\Gamma(k+\varsigma_2+1)\Gamma(i+\lambda)\, k!(i-k)!}. \tag{7}$$

The monomial terms τ^k can be stated as a finite linear combination of JPs $\mathrm{P}_{\ell,r}^{(\varsigma_1,\varsigma_2)}(\tau)$ in the following form:

$$\tau^k = \sum_{r=0}^{k} b_r^{(k)}(\ell)\, \mathrm{P}_{\ell,r}^{(\varsigma_1,\varsigma_2)}(\tau), \tag{8}$$

where we write the following:

$$b_r^{(k)}(\ell) = \frac{\ell^k\, k!\, (\lambda+2r)\Gamma(k+\varsigma_2+1)\Gamma(r+\lambda)}{(k-r)!\,\Gamma(r+\varsigma_2+1)\Gamma(k+r+\lambda+1)}. \tag{9}$$

3.2. Introducing Generalized FJFs

This portion focuses on introducing the set of GFJFs, $\mathrm{P}_{\ell,i}^{(\varsigma_1,\varsigma_2,\vartheta)}(\tau)$, $\vartheta > 0$, with some necessary properties needed throughout the paper. They are defined as follows [61]:

$$\mathrm{P}_{\ell,i}^{(\varsigma_1,\varsigma_2,\vartheta)}(\tau) = \sum_{k=0}^{i} c_k^{(i)} \left(\frac{\tau}{\ell}\right)^{\vartheta k}, \quad i = 0, 1, 2, \ldots. \tag{10}$$

This set has the following property:

Lemma 1 ([61]). *The set of GFJFs, $\{\mathrm{P}_{\ell,i}^{(\varsigma_1,\varsigma_2,\vartheta)}(\tau)\}_{i\geq 0}$, constitutes a complete orthogonal system on the subsequent space:*

$$L^2_{w_\ell^{\varsigma_1,\varsigma_2,\vartheta}} = \left\{ f \;\middle|\; f : [0,\ell] \to \mathbb{R}, \int_0^\ell w_\ell^{\varsigma_1,\varsigma_2,\vartheta}(\tau)\, |f(\tau)|^2\, d\tau < \infty \right\}, \tag{11}$$

considering the weight function $w_\ell^{\varsigma_1,\varsigma_2,\vartheta}(\tau) = \vartheta\, \tau^{\vartheta(\varsigma_2+1)-1}\, (\ell^\vartheta - \tau^\vartheta)^{\varsigma_1}$, i.e.,

$$\int_0^\ell w_\ell^{\varsigma_1,\varsigma_2,\vartheta}(\tau)\, \mathrm{P}_{\ell,n}^{(\varsigma_1,\varsigma_2,\vartheta)}(\tau)\, \mathrm{P}_{\ell,m}^{(\varsigma_1,\varsigma_2,\vartheta)}(\tau)\, d\tau = \begin{cases} 0, & m \neq n, \\ h_{\ell,n}^{(\varsigma_1,\varsigma_2,\vartheta)}, & m = n, \end{cases} \tag{12}$$

where $h_{\ell,n}^{(\varsigma_1,\varsigma_2,\vartheta)} = \ell^{\lambda\vartheta}\, 2^{-\lambda}\, h_n^{(\varsigma_1,\varsigma_2)}$.

The following inversion formula given in Lemma 2 is needed throughout the paper.

Lemma 2. *The relationship between $\tau^{\vartheta k}$ and the basis $\mathrm{P}_{\ell,r}^{(\varsigma_1,\varsigma_2,\vartheta)}(\tau)$ is given by the following:*

$$\tau^{\vartheta k} = \sum_{r=0}^{k} b_r^{(k)}(\ell^{\vartheta})\,\mathrm{P}_{\ell,r}^{(\varsigma_1,\varsigma_2,\vartheta)}(\tau), \quad k = 0,1,2,\ldots. \tag{13}$$

Proof. The result follows directly from application of formula (8), by replacing τ with $\tau^{\vartheta}\ell^{-\vartheta+1}$. □

New OFs $\{\phi_{n,j}^{(\varsigma_1,\varsigma_2,\vartheta)}(\tau)\}_{j\geq 0}$ are introduced, such as the following:

$$\phi_{n,j}^{(\varsigma_1,\varsigma_2,\vartheta)}(\tau) = \tau^{n}\mathrm{P}_{\ell,j}^{(\varsigma_1,\varsigma_2,\vartheta)}(\tau), \tag{14}$$

that satisfy the following:

$$\int_0^{\ell} w_{n,\ell}^{\varsigma_1,\varsigma_2,\vartheta}(\tau)\,\phi_{n,i}^{(\varsigma_1,\varsigma_2,\vartheta)}(\tau)\,\phi_{n,j}^{(\varsigma_1,\varsigma_2,\vartheta)}(\tau)\,d\tau = \begin{cases} 0, & i \neq j, \\ h_{\ell,i}^{(\varsigma_1,\varsigma_2,\vartheta)}, & i = j, \end{cases} \tag{15}$$

where $w_{n,\ell}^{\varsigma_1,\varsigma_2,\vartheta}(\tau) = \dfrac{1}{\tau^{2n}} w_{\ell}^{\varsigma_1,\varsigma_2,\vartheta}(\tau)$.

Remark 1. *Since we have*

$$\phi_{0,i}^{(\varsigma_1,\varsigma_2,\vartheta)}(\tau) = \mathrm{P}_{\ell,i}^{(\varsigma_1,\varsigma_2,\vartheta)}(\tau), \qquad \mathrm{P}_{\ell,i}^{(\varsigma_1,\varsigma_2,1)}(\tau) = \mathrm{P}_{\ell,i}^{(\varsigma_1,\varsigma_2)}(\tau), \qquad \phi_{0,i}^{(\varsigma_1,\varsigma_2,1)}(\tau) = \mathrm{P}_{\ell,i}^{(\varsigma_1,\varsigma_2)}(\tau),$$

so $\phi_{n,i}^{(\varsigma_1,\varsigma_2,\vartheta)}(\tau)$ are generalizations of $\mathrm{P}_{\ell,i}^{(\varsigma_1,\varsigma_2,\vartheta)}(\tau)$ and $\mathrm{P}_{\ell,i}^{(\varsigma_1,\varsigma_2)}(\tau)$. Additionally, there are also generalizations of $\mathrm{P}_{\ell,i}^{(\varsigma_1,\varsigma_2)}(\tau)$.

4. Operational Matrices for Both ODs and VOFDs of $\boldsymbol{\phi_{n,i}^{(\varsigma_1,\varsigma_2,\vartheta)}(\tau)}$

In this section, two main theorems are presented that provide the two operational matrices for ODs as well as VOFDs of the vector, written as follows:

$$\mathbf{\Phi}_{n,M}^{(\varsigma_1,\varsigma_2,\vartheta)}(\tau) = [\phi_{n,0}^{(\varsigma_1,\varsigma_2,\vartheta)}(\tau), \phi_{n,1}^{(\varsigma_1,\varsigma_2,\vartheta)}(\tau), \ldots, \phi_{n,M}^{(\varsigma_1,\varsigma_2,\vartheta)}(\tau)]^{T}. \tag{16}$$

Theorem 1. ${}_{0}^{LC}\mathbb{D}_{\tau}^{\nu(\tau)}\phi_{n,i}^{(\varsigma_1,\varsigma_2,\vartheta)}(\tau)$ *can be formulated in the following form:*

$${}_{0}^{LC}\mathbb{D}_{\tau}^{\nu(\tau)}\phi_{n,i}^{(\varsigma_1,\varsigma_2,\vartheta)}(\tau) := \frac{1}{\tau^{\nu(\tau)}}\sum_{j=0}^{i}\Theta_{i,j}^{(n,\vartheta)}(\nu(\tau))\phi_{n,j}^{(\varsigma_1,\varsigma_2,\vartheta)}(\tau), \tag{17}$$

and therefore, the VOFD of $\mathbf{\Phi}_{n,M}^{(\varsigma_1,\varsigma_2,\vartheta)}(\tau)$ has the following form:

$${}_{0}^{LC}\mathbb{D}_{\tau}^{\nu(\tau)}\mathbf{\Phi}_{n,M}^{(\varsigma_1,\varsigma_2,\vartheta)}(\tau) = \tau^{-\nu(\tau)}\mathbf{D}_{n}^{(\nu(\tau),\vartheta)}\mathbf{\Phi}_{n,M}^{(\varsigma_1,\varsigma_2,\vartheta)}(\tau), \tag{18}$$

where $\mathbf{D}_{n}^{(\nu(\tau),\vartheta)} = (d_{i,j}^{(n,\vartheta)}(\nu(\tau)))$ forms a matrix of size $(M+1)\times(M+1)$. Its explicit format is as follows:

$$\begin{pmatrix} \Theta_{0,0}^{(n,\vartheta)}(\nu(\tau)) & 0 & \cdots & \cdots & \cdots & 0 \\ \Theta_{1,0}^{(n,\vartheta)}(\nu(\tau)) & \Theta_{1,1}^{(n,\vartheta)}(\nu(\tau)) & 0 & \cdots & \cdots & 0 \\ \vdots & & \ddots & & & \vdots \\ \Theta_{i,0}^{(n,\vartheta)}(\nu(\tau)) & \cdots & \Theta_{i,i}^{(n,\vartheta)}(\nu(\tau)) & 0 & \cdots & 0 \\ \vdots & & & \ddots & & \vdots \\ \vdots & & & & \ddots & 0 \\ \Theta_{M,0}^{(n,\vartheta)}(\nu(\tau)) & \cdots & \cdots & \cdots & \cdots & \Theta_{N,M}^{(n,\vartheta)}(\nu(\tau)) \end{pmatrix}. \tag{19}$$

Here, we have the following:

$$d_{i,j}^{(n,\vartheta)}(\nu(\tau)) = \begin{cases} \Theta_{i,j}^{(n,\vartheta)}(\nu(\tau)), & i \geq j, \\ 0, & \text{otherwise}, \end{cases} \tag{20}$$

and

$$\Theta_{i,j}^{(n,\vartheta)}(\nu(\tau)) = \frac{(-1)^{i-j}(2j+\lambda)(\varsigma_2+1)_i(\lambda)_j}{(\varsigma_2+1)_j(\lambda)_i} \sum_{k=0}^{i-j} \frac{(-1)^k \Gamma(n+(j+k)\vartheta+1)\,\Gamma(i+j+k+\lambda)}{k!\,(i-j-k)!\,\Gamma(2j+k+\lambda+1)\,\Gamma(n-\nu(\tau)+(j+k)\vartheta+1)}. \tag{21}$$

Proof. On account of (10) and by utilizing (5a), one obtains the following:

$${}_0^{LC}\mathbb{D}_\tau^{\nu(\tau)} \phi_{n,i}^{(\varsigma_1,\varsigma_2,\vartheta)}(\tau) = \tau^{n-\nu(\tau)} \sum_{k=0}^{i} c_k^{(i)}\, \ell^{-k\vartheta} \frac{\Gamma(k\vartheta+n+1)}{\Gamma(k\vartheta+n-\nu(\tau)+1)} \tau^{k\vartheta}. \tag{22}$$

By employing (13) and (22) takes the form (17) which yields the following:

$${}_0^{LC}\mathbb{D}_\tau^{\nu(\tau)} \phi_{n,i}^{(\varsigma_1,\varsigma_2,\vartheta)}(\tau) = \tau^{-\nu(\tau)} \left[\Theta_{i,0}^{(n,\vartheta)}(\nu(\tau)), \Theta_{i,1}^{(n,\vartheta)}(\nu(\tau)), \ldots, \Theta_{i,i}^{(n,\vartheta)}(\nu(\tau)), 0, \ldots, 0\right] \mathbf{\Phi}_{n,M}^{(\varsigma_1,\varsigma_2,\vartheta)}(\tau), \tag{23}$$

and this expression proves (18). □

Theorem 2. *$D^m \phi_{n,i}^{(\varsigma_1,\varsigma_2,\vartheta)}(\tau)$ can be formulated as follows:*

$$D^m \phi_{n,i}^{(\varsigma_1,\varsigma_2,\vartheta)}(\tau) = \tau^{-m} \sum_{j=0}^{i} \Theta_{i,j}^{(n,\vartheta)}(m) \phi_{n,j}^{(\varsigma_1,\varsigma_2,\vartheta)}(\tau), \tag{24}$$

and as a consequence, the mth-derivatives of $\mathbf{\Phi}_{n,M}^{(\varsigma_1,\varsigma_2,\vartheta)}(\tau)$ has the following form:

$$D^m \mathbf{\Phi}_{n,M}^{(\varsigma_1,\varsigma_2,\vartheta)}(\tau) = \tau^{-m} \mathbf{D}_n^{(m,\vartheta)} \mathbf{\Phi}_{n,M}^{(\varsigma_1,\varsigma_2,\vartheta)}(\tau). \tag{25}$$

Proof. The proof follows analogous arguments to those presented in Theorem 1. □

For instance, if $M = 3$, $\varsigma_1 = \varsigma_2 = 0$, $m = 1$ and $\nu(\tau) = \tau$ we obtain the following:

$$\mathbf{D}_n^{(1,\vartheta)} = \begin{pmatrix} n & 0 & 0 & 0 \\ \vartheta & \vartheta+n & 0 & 0 \\ \vartheta & 3\nu & 2\vartheta+n & 0 \\ \vartheta & 3\vartheta & 5\vartheta & 3\vartheta+n \end{pmatrix}_{4\times 4}, \tag{26}$$

and

$$\mathbf{D}_n^{(\tau,\vartheta)} = \begin{pmatrix} \frac{\Gamma(n+1)}{\Gamma(n-\tau+1)} & 0 & 0 & 0 \\ \frac{\Gamma(n+\vartheta+1)}{\Gamma(n-\tau+\vartheta+1)} - \frac{\Gamma(n+1)}{\Gamma(n-\tau+1)} & \frac{\Gamma(n+\vartheta+1)}{\Gamma(n-\tau+\vartheta+1)} & 0 & 0 \\ -\frac{3\Gamma(n+\vartheta+1)}{\Gamma(n-\tau+\vartheta+1)} + \frac{2\Gamma(n+2\vartheta+1)}{\Gamma(n-\tau+2\vartheta+1)} + \frac{\Gamma(n+1)}{\Gamma(n-\tau+1)} & \frac{3\Gamma(n+2\vartheta+1)}{\Gamma(n-\tau+2\vartheta+1)} - \frac{3\Gamma(n+\vartheta+1)}{\Gamma(n-\tau+\vartheta+1)} & \frac{\Gamma(n+2\vartheta+1)}{\Gamma(n-\tau+2\vartheta+1)} & 0 \\ \frac{6\Gamma(n+\vartheta+1)}{\Gamma(n-\tau+\vartheta+1)} - \frac{10\Gamma(n+2\vartheta+1)}{\Gamma(n-\tau+2\vartheta+1)} + \frac{5\Gamma(n+3\vartheta+1)}{\Gamma(n-\tau+3\vartheta+1)} - \frac{\Gamma(n+1)}{\Gamma(n-\tau+1)} & \frac{6\Gamma(n+\vartheta+1)}{\Gamma(n-\tau+\vartheta+1)} - \frac{15\Gamma(n+2\vartheta+1)}{\Gamma(n-\tau+2\vartheta+1)} + \frac{9\Gamma(n+3\vartheta+1)}{\Gamma(n-\tau+3\vartheta+1)} & \frac{5\Gamma(n+3\vartheta+1)}{\Gamma(n-\tau+3\vartheta+1)} - \frac{5\Gamma(n+2\vartheta+1)}{\Gamma(n-\tau+2\vartheta+1)} & \frac{\Gamma(n+3\vartheta+1)}{\Gamma(n-\tau+3\vartheta+1)} \end{pmatrix}_{4\times 4}. \tag{27}$$

5. Numerical Handling for MTVOFDE Subject to ICs

Here, we utilize the OMs obtained in Theorems 1 and 2 to derive NUMSs for (1) and (2).

5.1. Homogeneous ICs

Suppose we have homogeneous initial conditions (HICs), i.e., $\omega_s = 0$, $s = 0, 1, 2, \ldots, n-1$. We propose the approximate solution (APPS) to $\chi(\tau)$ as follows:

$$\chi(\tau) \simeq \chi_M(\tau) = \sum_{i=0}^{M} c_i \, \phi_{n,i}^{(\varsigma_1,\varsigma_2,\vartheta)}(\tau) = \boldsymbol{A}^T \boldsymbol{\Phi}_{n,M}^{(\varsigma_1,\varsigma_2,\vartheta)}(\tau), \tag{28}$$

where $\boldsymbol{A} = [c_0, c_1, \ldots, c_M]^T$.

Two Theorems 1 and 2 enable us to obtain the following:

$${}_0^{LC}\mathbb{D}_\tau^{\nu(\tau)} \chi_M(\tau) = \begin{cases} \tau^{-\nu(\tau)} \, \boldsymbol{A}^T \mathbf{D}_n^{(\nu(\tau))} \boldsymbol{\Phi}_{n,M}^{(\varsigma_1,\varsigma_2,\vartheta)}(\tau), \ \nu(\tau) \text{ is a function or fraction number,} \\ \tau^{-m} \, \boldsymbol{A}^T \mathbf{D}_n^{(m)} \boldsymbol{\Phi}_{n,M}^{(\varsigma_1,\varsigma_2,\vartheta)}(\tau), \ \nu(\tau) = m, \quad m \text{ is an integer.} \end{cases} \tag{29}$$

By utilizing the approximations from (28) and (29), this method enables the representation of the residual in Equation (1):

$$\begin{aligned} R_{n,M}(\tau) = \ & \tau^{-\nu(\tau)} \, \boldsymbol{A}^T \mathbf{D}_n^{(\nu(\tau))} \boldsymbol{\Phi}_{n,M}^{(\varsigma_1,\varsigma_2,\vartheta)}(\tau) \\ & - F\Big(\tau, \boldsymbol{A}^T \boldsymbol{\Phi}_{n,M}^{(\varsigma_1,\varsigma_2,\vartheta)}(\tau), \tau^{-\nu_1(\tau)} \, \boldsymbol{A}^T \mathbf{D}_n^{(\nu_1)} \boldsymbol{\Phi}_{n,M}^{(\varsigma_1,\varsigma_2,\vartheta)}(\tau), \ldots, \tau^{-\nu_m(\tau)} \, \boldsymbol{A}^T \mathbf{D}_n^{(\nu_m)} \boldsymbol{\Phi}_{n,M}^{(\varsigma_1,\varsigma_2,\vartheta)}(\tau)\Big). \end{aligned} \tag{30}$$

We suggest a spectral approach, referred to as GFJCOPMM using SCM and the computed previous OMs. The collocation nodes for GFJCOPMM are the $(M+1)$ roots of $\mathrm{P}_{\ell,M+1}^{(\varsigma_1,\varsigma_2)}(\tau)$ or, alternatively, the points $\tau_j = \frac{\ell(j+1)}{M+2}, j = 0, 1, \ldots, M$ in such a way that the following is obtained:

$$R_{n,M}(\tau_j) = 0, \quad j = 0, 1, \ldots, M. \tag{31}$$

By solving (31) using Newton's iterative method, we obtain the desired NUMSs (28).

5.2. Nonhomogeneous ICs

Here, the GFJCOPMM is developed to solve the system given in Equations (1) and (2) by converting it into an equivalent formulation with (HICs). This conversion takes the following format:

$$\bar{\chi}(\tau) := \chi(\tau) - q_n(\tau), \quad q_n(\tau) = \sum_{i=0}^{n-1} \frac{\beta_i}{i!} \tau^i, \tag{32}$$

which leads to the following:

$$\begin{aligned} {}_0^{LC}\mathbb{D}_\tau^{\nu(\tau)} \bar{\chi}(\tau) = & -{}_0^{LC}\mathbb{D}_\tau^{\nu(\tau)} q_n(\tau) \\ & + F\Big(\tau, \bar{\chi}(\tau) + q_n(\tau), {}_0^{LC}\mathbb{D}_\tau^{\nu_1(\tau)}(\bar{\chi}(\tau) + q_n(\tau)), {}_0^{LC}\mathbb{D}_\tau^{\nu_2(\tau)}(\bar{\chi}(\tau) + q_n(\tau)), \ldots, {}_0^{LC}\mathbb{D}_\tau^{\nu_m(\tau)}(\bar{\chi}(\tau) + q_n(\tau))\Big), \end{aligned} \tag{33}$$

for $\tau \in [0, \ell]$, where for $j = 0, 1, \ldots, n-1$, we set the following:

$$\bar{\chi}^{(j)}(0) = 0. \tag{34}$$

Therefore, one obtains the following:

$$\chi_M(\tau) = \bar{\chi}_M(\tau) + q_n(\tau). \tag{35}$$

Remark 2. *The algorithm presented to solve multiple numerical examples in Section 7. The computations were performed using Mathematica 13.3 on a computer system equipped with an Intel(R) Core(TM) i9-10850 CPU operating at 3.60 GHz, featuring 10 cores and 20 logical processors. The algorithmic steps for solving the VO-MTFDEs using GFJCOPMM are expressed as in Algorithm 1.*

Algorithm 1 GFJCOPMM algorithm

Step 1. Given $\varsigma_1, \varsigma_2, \vartheta$, M, ν)), $\nu_i(\tau), i = 1, 2, \ldots, m$ and ω_s, $s = 0, 1, \ldots, n-1$.
Step 2. Define the basis $\phi_{n,i}^{(\varsigma_1,\varsigma_2,\vartheta)}(\tau)$, the vectors $\boldsymbol{A}$, $\boldsymbol{\Phi}_{n,M}^{(\varsigma_1,\varsigma_2,\vartheta)}(\tau)$ and compute the elements of $(M+1)(M+1)$ matrices $\mathbf{D}_n^{(\nu(\tau),\vartheta)}$, $\mathbf{D}_n^{(\nu_i(\tau),\vartheta)}$, $i = 0, 1, \ldots, m$.
Step 3. Evaluate $\boldsymbol{A}^T \mathbf{D}_n^{(\nu(\tau),\vartheta)} \boldsymbol{\Phi}_{n,M}^{(\varsigma_1,\varsigma_2,\vartheta)}(\tau)$ and $\boldsymbol{A}^T \mathbf{D}_n^{(\nu_i(\tau),\vartheta)} \boldsymbol{\Phi}_{n,M}^{(\varsigma_1,\varsigma_2,\vartheta)}(\tau)$, $i = 0, 1, \ldots, m$.
Step 4. Define $R_{n,M}(\tau)$ as in Equation (30).
Step 5. List $R_{n,M}(\tau_i) = 0$, $i = 0, 1, \ldots, M$, defined in Equation (31).
Step 6. Use Mathematica's built-in numerical solver to obtain the solution to the system of equations in [Output 5].
Step 7. Evaluate $\chi_M(\tau)$ defined in Equation (28) (In the case of HICs).
Step 8. Evaluate $q_n(\tau)$ and $\chi_M(\tau)$ defined in Equation (35) (In the case of Nonhomogeneous ICs).

Remark 3. *For interested readers, we utilized several built-in functions in Mathematica 13.3 for our numerical implementation of the provided algorithms. Below is a summary of the tools used, along with concise information about each function.*

Array: For creating and manipulating arrays, which are used to hold coefficients and operational matrices throughout the computations.
NSolve: For finding numerical solutions to nonlinear algebraic equations; it is utilized to compute the zeros of $\mathrm{P}_{\ell,M+1}^{(\varsigma_1,\varsigma_2)}(\tau)$ *or, alternatively, the points* $\tau_j = \frac{\ell(j+1)}{M+2}, j = 0, 1, \ldots, M$.
FindRoot: For solving equations by finding roots; it is essential in handling the nonlinear aspects of our system, using a zero initial approximation.
JacobiP: For generating $\phi_{n,i}^{(\varsigma_1,\varsigma_2,\vartheta)}(\tau)$*, which serve as basis functions that provide the foundation for approximating the solution in our collocation method.*
D: To compute ordinary derivatives to determine the defined residuals.
LCaputoD: To compute Liouville–Caputo fractional derivatives to determine the defined residuals.
Table: For generating lists and arrays of values based on specified formulas, particularly for collocation points and other parameterized data.

6. Error Analysis and Convergence Results

The following presents a thorough convergence analysis of the GFJCOPMM approach. With this respect, consider the following space:

$$W_{n,M} = Span\{\phi_{n,0}^{(\varsigma_1,\varsigma_2,\vartheta)}(\tau), \phi_{n,1}^{(\varsigma_1,\varsigma_2,\vartheta)}(\tau), \ldots, \phi_{n,M}^{(\varsigma_1,\varsigma_2,\vartheta)}(\tau)\}.$$

In addition, the absolute error (AE) between the true solution $\chi(\tau)$ and its approximation $\chi_M(\tau)$ is given by the following:

$$E_M(\tau) = |\chi(\tau) - \chi_M(\tau)|. \tag{36}$$

In this manuscript, the corresponding error obtained by GFJCOPMM is analyzed by using the L_2 norm, written as follows:

$$\|E_M\|_2 = \|\chi - \chi_M\|_2 = \left(\int_0^{\ell} |\chi(\tau) - \chi_M(\tau)|^2 \, d\tau \right)^{1/2}, \tag{37}$$

and the L_∞ (MAE) norm, written as follows:

$$\|E_M\|_\infty = \|\chi - \chi_M\|_\infty = \max_{\tau\in[0,\ell]} |\chi(\tau) - \chi_M(\tau)|. \tag{38}$$

Theorem 3. *Suppose that $\chi(\tau) = \tau^n u(\tau)$ be the actual solution and $\chi_M(\tau)$ its best possible approximation (BPA) from the subspace $W_{n,M}$ having the form (28). Then, there exists a constant $K = K(n, M) > 0$ such that the subsequent estimations hold:*

$$\|E_M\|_\infty \leq \frac{K\,\ell^{n+1}}{2^\lambda}\Big(\frac{e\,\ell}{4}\Big)^M (M+1)^{q-M-1}, \tag{39}$$

and

$$\|E_M\|_2 \leq \frac{K\,\ell^{2n+3/2}}{2^\lambda}\Big(\frac{e\,\ell}{4}\Big)^M (M+1)^{q-M-1}, \tag{40}$$

where $K = \max\limits_{\tau\in[0,\ell]}\Big|\dfrac{d^{M+1}\,u(\eta)}{d\,\tau^{M+1}}\Big|$, $\eta \in [0,\ell]$, and $q = \max\{-\frac{1}{2}, \varsigma_1, \varsigma_2\} < M+1$.

Proof. In view of Theorem 3.3 in the book (p.109) in [62], $u(\tau)$ takes the subsequent representation:

$$u(\tau) = u_M(\tau) + \frac{K}{(M+1)!}\prod_{k=0}^{M}(\tau - \tau_k), \tag{41}$$

where $u_M(\tau)$ represents the polynomial interpolation operator applied to $u(\tau)$ at the points τ_k for $k = 0, 1, \ldots, M$, that staisfy $\mathrm{P}^{(\varsigma_1,\varsigma_2)}_{\ell,M+1}(\tau_k) = 0$ such that $M > q-1$. Then we obtain the following:

$$\|u - u_M\|_\infty \leq \frac{K}{(M+1)!}\Big\|\prod_{k=0}^{M}(\tau - \tau_k)\Big\|_\infty = \frac{K}{(M+1)!\,c^{M+1}_{M+1}}\|\mathrm{P}^{(\varsigma_1,\varsigma_2)}_{\ell,M+1}(\tau)\|_\infty, \tag{42}$$

where $c^{M+1}_{M+1} = \dfrac{\Gamma(2M+\lambda+2)}{\ell^{M+1}\,(M+1)!\,\Gamma(M+\lambda+1)}$.
Applying the identity from (formula (7.32.2)) in [60], we derive the following:

$$\|\mathrm{P}^{(\varsigma_1,\varsigma_2)}_{\ell,M+1}\|_\infty \simeq (M+1)^q, \tag{43}$$

hence the following:

$$\|u - u_M\|_\infty \leq K\frac{\ell^{M+1}\Gamma(M+\lambda+1)(M+1)^q}{\Gamma(2M+\lambda+2)}, \tag{44}$$

By using [63] we obtain the following:

$$\Gamma(r+\lambda) = \mathcal{O}\,(r^{\lambda-1}\,r!), \quad r! = \mathcal{O}\Big(\sqrt{2\pi\,r}\,\Big(\frac{r}{e}\Big)^r\Big), \quad (2r)! = \frac{1}{\sqrt{\pi}}\,4^r\,r!\,\Gamma(r+1/2), \tag{45}$$

and through algebraic manipulation, inequality (44) reduces to the following expression:

$$\|u - u_M\|_\infty \leq \frac{K\,\ell}{2^\lambda}\Big(\frac{e\,\ell}{4}\Big)^M (M+1)^{q-M-1}. \tag{46}$$

Let us set $\chi(\tau) \simeq Y_M(\tau) = \tau^n u_M(\tau)$, to arrive at the following:

$$\|\chi - Y_M\|_\infty \leq \ell^n\|u - u_M\|_\infty \leq \frac{K\,\ell^{n+1}}{2^\lambda}\Big(\frac{e\,\ell}{4}\Big)^M (M+1)^{q-M-1}. \tag{47}$$

Since the APPS $\chi_M(\tau) \in W_{n,M}$ shows the BPA to $\chi(\tau)$, one arrives at the following:

$$\|\chi - \chi_M\|_\infty \leq \|\chi - g\|_\infty, \quad \forall g \in W_{n,M}, \tag{48}$$

and

$$\|\chi - \chi_M\|_2 \leq \|\chi - g\|_2, \quad \forall g \in W_{n,M}. \tag{49}$$

Therefore, we obtain the following:

$$\|\chi - \chi_M\|_\infty \leq \|\chi - Y_M\|_\infty \leq \left(\frac{e\,\ell}{4}\right)^M \frac{K\,\ell^{n+1}}{2^\lambda}(M+1)^{q-M-1}, \tag{50}$$

and

$$\|\chi - \chi_M\|_2 \leq \|\chi - Y_M\|_2 \leq \ell^n \|u - u_M\|_2 = \ell^n \sqrt{\int_0^\ell |u(\tau) - u_M(\tau)|^2\, d\tau} \leq \frac{K\,\ell^{2n+3/2}}{2^\lambda}\left(\frac{e\,\ell}{4}\right)^M (M+1)^{q-M-1}. \tag{51}$$

□

The following implication establishes the rapid convergence of the approximation errors:

Corollary 1. *The subsequent estimations hold for all $M > q - 1$:*

$$\|E_M\|_\infty = \mathcal{O}((e\,\ell/4)^M\, M^{q-M-1}), \tag{52}$$

and

$$\|E_M\|_2 = \mathcal{O}((e\,\ell/4)^M\, M^{q-M-1}). \tag{53}$$

The theorem presented below illustrates the stability of errors, specifically regarding error propagation calculations.

Theorem 4. *Given any two iterative estimates of $\chi(\tau)$, the result is as follows:*

$$|\chi_{M+1} - \chi_M| = \mathcal{O}((e\,\ell/4)^M\, M^{q-M-1}), \tag{54}$$

Proof. We have the following:

$$|\chi_{M+1} - \chi_M| = |\chi_{M+1} - \chi + \chi - \chi_M| \leq |\chi - \chi_{M+1}| + |\chi - \chi_M| \leq \|E_{M+1}\|_\infty + \|E_M\|_\infty, \tag{55}$$

By considering (52), we can obtain (54). □

7. Numerical Simulations

In this portion, numerical computations are provided to illustrate that GFJCOPMM has high efficiency. In these examples, we show that the GFJCOPMM provides spectrally exact solutions for problems admitting polynomial solutions of degree N or less, as verified numerically in Examples 1–4. The method achieves exact solutions for select non-polynomial cases where the true solution can be represented exactly by the chosen basis, as verified in Example 5.

Tables 1, 2, 4, and 5 demonstrate the superior accuracy of GFJCOPMM, with computed errors significantly smaller than those obtained by existing methods [17–19,21,36,49]. In addition, Table 3 presents the computed error norms for the numerical solutions $\chi_M(\tau)$ obtained via GFJCOPMM. Furthermore, Figures 1–3 exhibit excellent visual agreement between actual and approximate solutions in Example 4.

Example 1. *Consider DE [17,18], as follows:*

$$\begin{cases} {}_0^{LC}\mathbb{D}_\tau^{2\tau}\chi(\tau) + \tau^{1/2}\,{}_0^{LC}\mathbb{D}_\tau^{\tau/3}\chi(\tau) + \tau^{1/3}\,{}_0^{LC}\mathbb{D}_\tau^{\tau/4}\chi(\tau) + \tau^{1/4}\,{}_0^{LC}\mathbb{D}_\tau^{\tau/5}\chi(\tau) + \tau^{1/5}\chi(\tau) = f(\tau), \quad \tau \in [0,\ell], \\ \chi(0) = 2, \quad \textit{and} \quad \chi'(0) = 0. \end{cases} \tag{56}$$

Here, the forcing function $f(\tau)$ is specifically selected to have the actual true solution $\chi(\tau) = 2 - \frac{\tau^2}{2}$.

By utilizing of *GFJCOPMM*, we reach the following:

$$\chi(\tau) = \chi_0(\tau) = c_0\,\phi_{2,0}^{(\varsigma_1,\varsigma_2,\vartheta)}(\tau) + 2,$$

where $c_0 = -1/2$.

Table 1. Supremum norm error $\|E_M\|_\infty$ comparison: GFJCOPMM versus reference methods [17,18] in Example 1.

	GFJCOPMM	**Method in [18]**			**Method in [17]**		
ℓ	$M=0$	$M=3$	$M=4$	$M=5$	$M=3$	$M=4$	$M=5$
1	0	0	0	0	0	2.2204×10^{-16}	2.2204×10^{-16}
2	0	0	0	0	0	4.4409×10^{-16}	1.3323×10^{-15}
4	0	0	0	0	2.2204×10^{-16}	3.5527×10^{-15}	3.1974×10^{-14}

Example 2. *In the second test problem, we consider Bagley–Torvik equation [18,64], written as follows:*

$$\begin{cases} D^2\chi(\tau) + {}_0^{LC}\mathbb{D}_\tau^{3/2}\chi(\tau) + \chi(\tau) = \tau^2 + 4\sqrt{\tau/\pi} + 2, \quad \tau \in [0,\ell], \\ \chi(0) = 0, \quad \chi'(0) = 0. \end{cases} \tag{57}$$

One can easily show that the actual solution is $\chi(\tau) = \tau^2$. Applying GFJCOPMM produces the following:

$$\chi(\tau) = \chi_0(\tau) = c_0\,\phi_{2,0}^{(\varsigma_1,\varsigma_2,\vartheta)}(\tau),$$

where $c_0 = 1$.

Remark 4. *It is worthy to note that the true actual solution of (57) when $M = 0$, $\varsigma_1, \varsigma_2 > -1$, while the researchers in [18], gave it was when $M = 2$. Moreover, in [64], it was gotten when $M \to \infty$, the best error was 2×10^{-10}.*

Example 3. *Consider the DE of the following form [18,19,21]:*

$$\begin{cases} {}_0^{LC}\mathbb{D}_\tau^{\nu(\tau)}\chi(\tau) - 10\,D\chi(\tau) + \chi(\tau) = 10\Big(\dfrac{\tau^{2-\nu(\tau)}}{\Gamma(3-\nu(\tau))} + \dfrac{\tau^{1-\nu(\tau)}}{\Gamma(2-\nu(\tau))}\Big) + 5\,\tau^2 - 90\ - \tau - 95, \\ \chi(0) = 5, \quad \chi'(0) = 10. \end{cases} \tag{58}$$

Here $\tau \in [0,1]$ and we have $\nu(\tau) = \dfrac{\tau + 2e^\tau}{7}$ and $\chi(\tau) = 5(\tau+1)^2$. Applying the GFJCOPMM leads to the following:

$$\chi(\tau) = \chi_0(\tau) = c_0\,\phi_{2,0}^{(\varsigma_1,\varsigma_2,\vartheta)}(\tau) + 5 + 10\,\tau,$$

where $c_0 = 5$.

Table 2. Supremum norm error $\|E_M\|_\infty$ comparison: GFJCOPMM versus reference methods [18,19,21] in Example 3.

τ	GFJCOPMM ($M=0$)	Ref. [21] ($M=4$)	Ref. [19] ($M=2$)	Ref. [18] ($M=2$)
0.2	0	8.091305×10^{-12}	1.818101×10^{-12}	0
0.4	0	2.024535×10^{-12}	1.817213×10^{-12}	8.881784×10^{-16}
0.6	0	9.564669×10^{-12}	1.820765×10^{-12}	1.776356×10^{-15}
0.8	0	1.696030×10^{-12}	1.818989×10^{-12}	1.776356×10^{-15}
1.0	0	1.734222×10^{-12}	1.818989×10^{-12}	0

Example 4. *Let us pay attention to the following nonlinear initial value problem [36,65]:*

$$\begin{cases} {}_0^{LC}\mathbb{D}_\tau^{\nu(\tau)}\chi(\tau)+\sin(\tau)\,\chi^2(\tau)=\dfrac{\Gamma(9/2)\,\tau^{7/2-\nu(\tau)}}{\Gamma(9/2-\nu(\tau))}+\sin(\tau)\,\tau^7, \quad 0<\nu(\tau)\le 1,\ \tau\in[0,1], \\ \chi(0)=0,\ \nu(\tau)=1-0.5\,e^{-\tau}, \end{cases} \tag{59}$$

with the actual solution given by $\chi(\tau)=\tau^{7/2}$.

Table 3 shows that the application of GFJCOPMM using $\vartheta=0.5$, $M=5$ *and various values of* ς_1 *and* ς_2 *leads to accuracy* 10^{-15} *and* 10^{-16}. *For example, using* $\varsigma_1=1/2$, $\varsigma_2=-1/2$, *the NUMSs* $\chi_5(\tau)$ *has the following form:*

$$\begin{aligned}\chi_5(\tau)=\,&2.61735\times10^{-14}\,\tau-2.38032\times10^{-13}\,\tau^{3/2}+8.20011\times10^{-13}\,\tau^2-1.36069\times10^{-12}\,\tau^{5/2}\\&+1.09202\times10^{-12}\,\tau^3+\tau^{7/2},\end{aligned}$$

with $\|E_5\|_\infty=7.78\times10^{-16}$.

Remark 5. *To better understand the effectiveness of the proposed method, we have included Figures 4 and 5, which utilize larger time intervals. We believe these new figures enhance the comparison analysis and provide clearer insights into the performance and robustness of our methodology across different scenarios.*

Table 3. MAEs for Example 4 using different values for ς_1, ς_2 and M and $\vartheta=0.5$.

ς_1	ς_2	*Errors*	$M=1$	$M=2$	$M=3$	$M=4$	$M=5$	$M=6$
0	0	$\|E_M\|_\infty$	1.29×10^{-1}	3.00×10^{-2}	4.85×10^{-3}	5.55×10^{-4}	1.00×10^{-15}	1.33×10^{-16}
		$\|E_M\|_2$	7.49×10^{-2}	1.71×10^{-2}	2.47×10^{-3}	1.81×10^{-4}	5.51×10^{-16}	5.14×10^{-16}
		CPU time	0.133	0.301	0.402	0.431	0.445	0.551
1	1	$\|E_M\|_\infty$	1.92×10^{-1}	3.31×10^{-2}	9.18×10^{-3}	1.11×10^{-3}	5.00×10^{-16}	7.76×10^{-16}
		$\|E_M\|_2$	5.73×10^{-2}	1.54×10^{-2}	3.42×10^{-3}	3.63×10^{-4}	3.54×10^{-16}	3.51×10^{-16}
		CPU time	0.124	0.313	0.404	0.426	0.428	0.514
$-1/2$	$1/2$	$\|E_M\|_\infty$	1.67×10^{-1}	5.47×10^{-2}	1.25×10^{-2}	1.35×10^{-3}	8.88×10^{-16}	7.77×10^{-16}
		$\|E_M\|_2$	9.90×10^{-2}	2.42×10^{-2}	4.32×10^{-3}	3.92×10^{-4}	5.15×10^{-16}	2.50×10^{-16}
		CPU time	0.120	0.309	0.398	0.410	0.419	0.497
$1/2$	$-1/2$	$\|E_M\|_\infty$	1.44×10^{-1}	2.72×10^{-2}	7.10×10^{-3}	8.46×10^{-4}	7.78×10^{-16}	7.78×10^{-16}
		$\|E_M\|_2$	5.43×10^{-2}	1.33×10^{-2}	2.41×10^{-3}	2.31×10^{-4}	6.50×10^{-16}	6.33×10^{-16}
		CPU time	0.129	0.381	0.422	0.443	0.447	0.552

Table 4. Supremum norm error $\|E_M\|_\infty$ comparison: GFJCOPMM versus reference methods [36] in Example 4.

	GFJCOPMM ($\varsigma_1 = 0$, $\varsigma_2 = 0$, $\vartheta = 0.5$)			**[36]**		
τ	$M = 2$	$M = 6$	$M = 10$	$M = 2$	$M = 6$	$M = 10$
0.2	3.18×10^{-4}	1.06×10^{-16}	5.81×10^{-17}	5.69×10^{-3}	9.75×10^{-6}	8.06×10^{-7}
0.4	1.37×10^{-4}	1.25×10^{-16}	1.25×10^{-17}	2.34×10^{-3}	8.02×10^{-6}	6.34×10^{-7}
0.6	1.22×10^{-4}	1.11×10^{-16}	0	2.78×10^{-3}	7.03×10^{-6}	5.53×10^{-7}
0.8	2.18×10^{-4}	1.11×10^{-16}	5.00×10^{-17}	2.52×10^{-3}	5.97×10^{-6}	4.59×10^{-7}
1.0	1.16×10^{-4}	4.44×10^{-16}	1.11×10^{-17}	1.66×10^{-2}	2.89×10^{-5}	1.95×10^{-6}

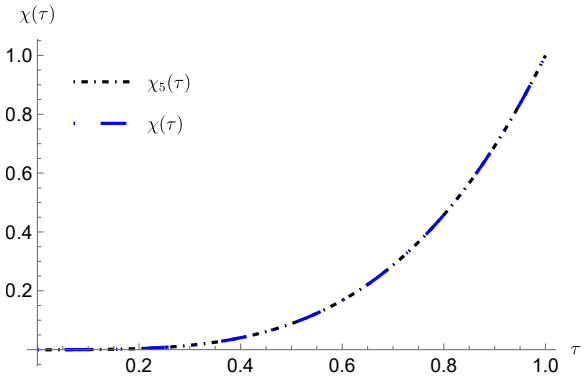


Figure 1. The profile of approximate and actual solutions in Example 4 using $\varsigma_1 = 1/2$, $\varsigma_2 = -1/2, \vartheta = 0.5$.

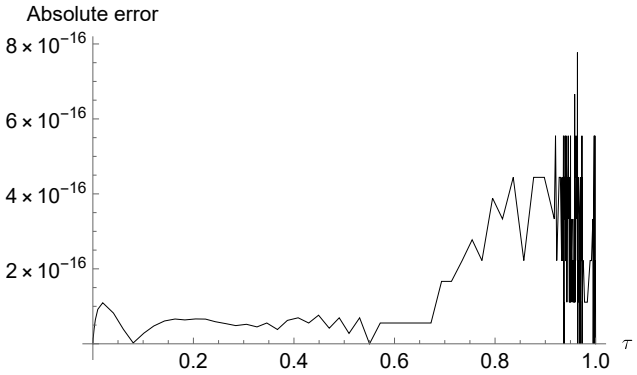


Figure 2. The AE $E_5(\tau)$ using $\varsigma_1 = 1/2, \varsigma_2 = -1/2, \vartheta = 0.5$ for Example 4.

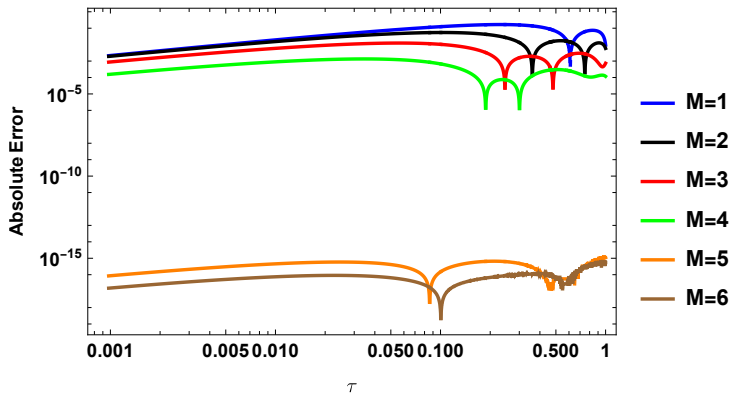


Figure 3. AEs $E_M(\tau)$ using various M and $\varsigma_1 = 1/2, \varsigma_2 = -1/2, \vartheta = 0.5$ for Example 4.

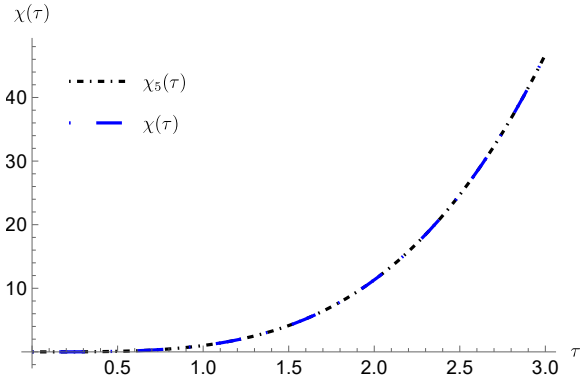


Figure 4. The profile of approximate and actual solutions ($\tau \in [0,3]$) in Example 4 using $\varsigma_1 = 1/2, \varsigma_2 = -1/2$, and $\vartheta = 0.5$.

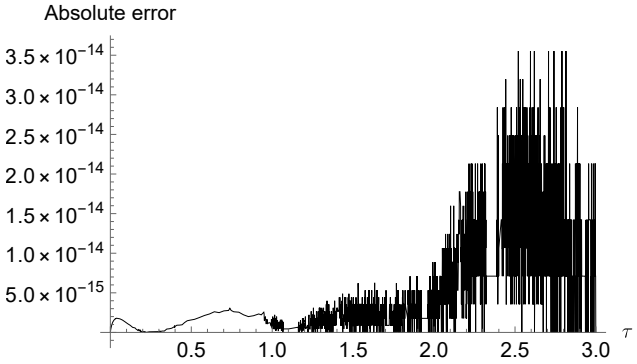


Figure 5. The AE $E_5(\tau)$, $\tau \in [0,3]$, using $\varsigma_1 = 1/2, \varsigma_2 = -1/2, \vartheta = 0.5$ for Example 4.

Example 5. *The last example is a DE of the following form [49]:*

$$\begin{cases} {}_0^{LC}\mathbb{D}_\tau^\gamma \chi(\tau) + (\chi(\tau))^2 = t + \left(\dfrac{\tau^{\gamma+1}}{\Gamma(\gamma+2)}\right)^2, \quad \gamma \in (0,1], \quad \tau \in [0,1], \\ \chi(0) = 0, \end{cases} \tag{60}$$

where $\chi(\tau) = \dfrac{\tau^{\gamma+1}}{\Gamma(\gamma+2)}$ *is the true solution. The application of GFJCOPMM gives us the following:*

$$\chi(\tau) = \chi_1(\tau) = c_0\, \phi_{1,0}^{(\varsigma_1,\varsigma_2,\gamma)}(\tau) + c_1\, \phi_{1,1}^{(\varsigma_1,\varsigma_2,\gamma)}(\tau),$$

where $c_0 = \dfrac{\varsigma_2 + 1}{(\lambda+1)\Gamma(\gamma+2)}$ *and* $c_1 = \dfrac{1}{(\lambda+1)\Gamma(\gamma+2)}$.

Table 5. Supremum norm error $\|E_M\|_\infty$ comparison: GFJCOPMM versus reference methods [49] in Example 5.

	GFJCOPMM $(M = 1)$	**Ref. [49] (k = 2 and M = 7)**	
τ	$\vartheta = \gamma =$ **0.5, 0.8**	$\gamma =$ **0.5**	$\gamma =$ **0.8**
0.0	0	8.43745×10^{-10}	1.26942×10^{-5}
0.1	0	1.42121×10^{-9}	2.00086×10^{-6}
0.2	0	1.95085×10^{-9}	2.94462×10^{-6}
0.3	0	1.95085×10^{-8}	2.86427×10^{-6}
0.4	0	1.47103×10^{-8}	1.51048×10^{-6}
0.5	0	1.13654×10^{-8}	3.96870×10^{-4}
0.6	0	8.98023×10^{-9}	3.60302×10^{-4}
0.7	0	7.46806×10^{-9}	3.23654×10^{-4}
0.8	0	6.97788×10^{-9}	2.85101×10^{-4}
0.9	0	7.78465×10^{-9}	2.39836×10^{-4}
1.0	0	1.02211×10^{-8}	1.76092×10^{-4}

Remark 6. *In view of the presented CPU time (in seconds), our approach has efficient performance. The calculations show that the memory consumption was excellent. For example, Table 3 shows that the calculated CPU time using $M = 6$ is 10% slower than $M = 3$ and, moreover, requires increasing 25% of memory consumption of RAM compared to the $M = 3$ calculation. The numerical examples and comparisons provided in our paper highlight the superior accuracy and efficiency of our algorithm, solidifying its potential for solving VO-MTFDEs effectively. In contrast, the methods described in [17–19,21,36,49] did not provide CPU time or memory usage data. However, our analysis suggests that our approach performs better than these referenced methods.*

Remark 7. *Our experiments indicate that the performance of the proposed methodology is relatively stable across a range of values for the parameters $\varsigma_1, \varsigma_2, \vartheta$, as we show in Table 3, allowing for flexibility in their selection based on specific problem requirements. Furthermore, we suggest that practitioners can conduct preliminary tests with varying parameter values to determine the most suitable configuration for their particular applications. This approach ensures that users can tailor the methodology to their needs while still achieving effective results.*

8. Conclusions

In this work, we introduced Generalized Fractional Jacobi Functions (GFJFs) that inherently satisfy the given initial conditions. By combining these functions with operational matrices (OMs) in a spectral collocation method (SCM), we develop the Generalized Fractional Jacobi Collocation Operational Matrix Method (GFJCOPMM). This approach yields highly accurate numerical solutions (NUMSs) with computational efficiency. However, it is important to acknowledge some limitations of the proposed method. The performance of GFJCOPMM may be sensitive to the selection of parameters, such as $\varsigma_1, \varsigma_2, \vartheta$, which can affect the accuracy of the solutions. Additionally, while the method shows promise for a range of FDEs, its applicability to highly nonlinear or complex boundary value problems remains to be fully explored. Future work will extend GFJCOPMM to boundary value problems. Moreover, the theoretical framework presented here can be generalized to solve broader classes of FDEs, such as the following: variable-order fractional systems, multi-term fractional operators, and nonlinear fractional PDEs under diverse initial/boundary conditions.

Author Contributions: Conceptualization, H.M.A., M.I. and C.C.; methodology, H.M.A., M.I., and C.C.; software, H.M.A.; validation, H.M.A., M.I., and C.C.; formal analysis, H.M.A., M.I., and C.C.; funding acquisition, C.C.; investigation, H.M.A., M.I., and C.C.; writing—original draft preparation, H.M.A. and M.I.; writing—review and editing, H.M.A., M.I., and C.C. All authors have read and agreed to the published version of the manuscript.

Funding: This research received no external funding.

Data Availability Statement: All data generated or analyzed during this study are included in this article.

Acknowledgments: The authors would like to thank the anonymous Reviewers and Editor for providing helpful comments and suggestions which further improved this work.

Conflicts of Interest: The authors declare no conflicts of interest.

References

1. Maayah, B.; Arqub, O.A.; Alnabulsi, S.; Alsulami, H. Numerical solutions and geometric attractors of a fractional model of the cancer-immune based on the Atangana-Baleanu-Caputo derivative and the reproducing kernel scheme. *Chin. J. Phys.* **2022**, *80*, 463–483. [CrossRef]
2. Berredjem, N.; Maayah, B.; Arqub, O.A. A numerical method for solving conformable fractional integro-differential systems of second-order, two-points periodic boundary conditions. *Alex. Eng. J.* **2022**, *61*, 5699–5711. [CrossRef]

3. Arqub, O.A.; Rabah, A.B.; Momani, S. A spline construction scheme for numerically solving fractional Bagley-Torvik and Painlevé models correlating initial value problems concerning the Caputo-Fabrizio derivative approach. *Int. J. Mod. Phys. C.* **2023**, *34*, 2350115. [CrossRef]
4. Almeida, R.; Tavares, D.; Torres, D.F.M. *The Variable-Order Fractional Calculus of Variations*; Springer: Cham, Switzerland, 2019.
5. Odzijewicz, T.; Malinowska, A.B.; Torres, D.F.M. Noether's theorem for fractional variational problems of variable order. *Cent. Eur. J. Phys.* **2013**, *11*, 691–701. [CrossRef]
6. Chen, S.; Liu, F.; Burrage, K. Numerical simulation of a new two-dimensional variable-order fractional percolation equation in non-homogeneous porous media. *Comput. Math. Appl.* **2014**, *67*, 1673–1681. [CrossRef]
7. Samko, S.G.; Ross, B. Integration and differentiation to a variable fractional order. *Integr. Transf. Spec. Funct.* **1993**, *1*, 277–300. [CrossRef]
8. Coimbra, C.F.M.; Soon, C.M.; Kobayashi, M.H. The variable viscoelasticity operator. *Ann. Phys.* **2005**, *14*, 378–389.
9. Ostalczyk, P.W.; Duch, P.; Brzeziński, D.W.; Sankowski, D. Order Functions Selection in the Variable-Fractional-Order PID Controller. In *Advances in Modelling and Control of Non-Integer-Order Systems*; Lecture Notes in Electrical Engineering; Springer: Berlin/Heidelberg, Germany, 2015; Volume 320, pp. 159–170.
10. Rapaić, M.R.; Pisano, A. Variable-order fractional operators for adaptive order and parameter estimation. *IEEE Trans. Autom. Contr.* **2013**, *59*, 798–803. [CrossRef]
11. Izadi, M.; Yüzbaşı, Ş.; Adel, W. Two novel Bessel matrix techniques to solve the squeezing flow problem between infinite parallel plates. *Comput. Math. Math. Phys.* **2021**, *61*, 2034–2053. [CrossRef]
12. Patnaik, S.; Semperlotti, F. Variable-order particle dynamics: Formulation and application to the simulation of edge dislocations. *Philos. Trans. R. Soc. A* **2020**, *378*, 20190290. [CrossRef]
13. Blaszczyk, T.; Bekus, K.; Szajek, K.; Sumelka, W. Approximation and application of the Riesz-Caputo fractional derivative of variable order with fixed memory. *Meccanica* **2022**, *57*, 861–870. [CrossRef]
14. Sheikhi, S.; Matinfar, M.; Firoozjaee, M.A. Numerical solution of variable-order differential equations via the Ritz approximation method by shifted Legendre polynomials. *Int. J. Appl. Comput. Math.* **2021**, *7*, 22. [CrossRef]
15. Abbasi, Z.; Izadi, M.; Hosseini, M.M. A highly accurate matrix method for solving a class of strongly nonlinear BVP arising in modeling of human shape corneal. *Math. Methods Appl. Sci.* **2023**, *46*, 1511–1527. [CrossRef]
16. Izadi, M.; Sene, N.; Adel, W.; El-Mesady, A. The Layla and Majnun mathematical model of fractional order: Stability analysis and numerical study. *Results Phys.* **2023**, *51*, 106650. [CrossRef]
17. Liu, J.; Li, X.; Wu, L. An operational matrix of fractional differentiation of the second kind of Chebyshev polynomial for solving multiterm variable order fractional differential equation. *Math. Probl. Eng.* **2016**, *2016*, 7126080. [CrossRef]
18. El-Sayed, A.A.; Baleanu, D.; Agarwal, P. A novel Jacobi operational matrix for numerical solution of multi-term variable-order fractional differential equations. *J. Taibah Univ. Sci.* **2020**, *14*, 963–974. [CrossRef]
19. Nagy, A.M.; Sweilam, N.H.; El-Sayed, A.A. New operational matrix for solving multiterm variable order fractional differential equations. *J. Comput. Nonlinear Dyn.* **2018**, *13*, 011001. [CrossRef]
20. Wang, L.F.; Ma, Y.P.; Yang, Y.Q. Legendre polynomials method for solving a class of variable order fractional differential equation. *CMES-Comp. Model. Eng.* **2014**, *101*, 97–111.
21. Chen, Y.M.; Wei, Y.Q.; Liu, D.Y.; Yu, H. Numerical solution for a class of nonlinear variable order fractional differential equations with Legendre wavelets. *Appl. Math. Lett.* **2015**, *46*, 83–88. [CrossRef]
22. Heydari, M.H.; Hooshmandasl M.R.; Cattani, C.; Hariharan, G. An optimization wavelet method for multi variable-order fractional differential equations. *Fundam. Inform.* **2017**, *151*, 255–273. [CrossRef]
23. Moustafa, M.; Youssri, Y.H.; Atta, A.G. Explicit Chebyshev Petrov–Galerkin scheme for time-fractional fourth-order uniform Euler–Bernoulli Pinned–Pinned beam equation. *Nonlinear Eng.* **2023**, *12*, 20220308. [CrossRef]
24. Youssri, Y.H.; Atta, A.G. Fejér-quadrature collocation algorithm for solving fractional integro-differential equations via Fibonacci polynomials. *Contemp. Math.* **2024**, *5*, 296–308. [CrossRef]
25. Ahmed, H.M. A new first finite class of classical orthogonal polynomials operational matrices: An application for solving fractional differential equations. *Contemp. Math.* **2023**, *4*, 974–994. [CrossRef]
26. Iqbal, S.; Francisco M.; Mohammed K.A.K.; Mohammad, E.S. A novel Elzaki transform homotopy perturbation method for solving time-fractional non-linear partial differential equations. *Bound. Value Probl.* **2022**, *2022*, 91. [CrossRef]
27. Martínez, F.; Mohammed K.A.K. On the Martínez–Kaabar fractal–fractional reduced Pukhov differential transformation and its applications. *Mathematics* **2025**, *13*, *352*. [CrossRef]
28. Hafez, R.M.; Youssri H.Y. Legendre-collocation spectral solver for variable-order fractional functional differential equations. *Comput. Methods Differ. Equ.* **2020**, *8*, 99–110.
29. Mallawi, F.; Alzaidy, J.F.; Hafez, R.M. Application of a Legendre collocation method to the space–time variable fractional-order advection–dispersion equation. *J. Taibah Uni. Sci.* **2019**, *13*, 324–330. [CrossRef]

30. Hafez, R.M.; Youssri, Y.H. Jacobi collocation scheme for variable-order fractional reaction-subdiffusion equation. *Comput. Appl. Math.* **2018**, *37*, 5315–5333. [CrossRef]
31. Bhrawy, A.H.; Taha, T.M.; Abdelkawy, M.A.; Hafez, R.M. On numerical methods for fractional differential equation on a semi-infinite interval. In *Fractional Dynamics*; Sciendo Migration: Warsaw, Poland, 2015; pp. 191–218.
32. Bushnaq, S.; Shah, K.; Tahir, S.; Ansari, K.J.; Sarwar, M.; Abdeljawad, T. Computation of numerical solutions to variable order fractional differential equations by using non-orthogonal basis. *AIMS Math.* **2022**, *7*, 10917–10938. [CrossRef]
33. Chen, Y.M.; Liu, L.Q.; Li, B.F.; Sun, Y. Numerical solution for the variable order linear cable equation with Bernstein polynomials. *Appl. Math. Comput.* **2014**, *238*, 329–341. [CrossRef]
34. Shen, S.; Liu, F.; Chen, J.; Turner, I.; Anh, V. Numerical techniques for the variable order time fractional diffusion equation. *Appl. Math. Comput.* **2012**, *218*, 10861–10870. [CrossRef]
35. Moghaddam, B.P.; Machado, J.A.T. Extended algorithms for approximating variable order fractional derivatives with applications. *J. Sci. Comput.* **2017**, *71*, 1351–1374. [CrossRef]
36. Nemati, S.; Pedro M.L.; Delfim F.M.T. Numerical solution of variable-order fractional differential equations using Bernoulli polynomials. *Fractal Fract.* **2021**, *5*, 219. [CrossRef]
37. Shen, J.; Tang, T.; Wang, L. *Spectral Methods: Algorithms, Analysis and Applications*; Springer: Berlin, Germany, 2011; Volume 41.
38. Ashry, H.; Abd-Elhameed, W.M.; Moatimid, G.M.; Youssri, Y.H. Robust shifted Jacobi-Galerkin method for solving linear hyperbolic telegraph type equation. *Palestine J. Math.* **2022**, *11*, 504–518.
39. Abd-Elhameed, W.M.; Ahmed, H.M.; Youssri, Y.H. A new generalized Jacobi Galerkin operational matrix of derivatives: Two algorithms for solving fourth-order boundary value problems. *Adv. Differ. Equ.* **2016**, *2016*, 22. [CrossRef]
40. Sabermahani, S.; Ordokhani, H.; Hassani, H. General Lagrange scaling functions: Application in general model of variable order fractional partial differential equations. *Comput. Appl. Math* **2021**, *40*, 269. [CrossRef]
41. Ahmed, H.M. Enhanced shifted Jacobi operational matrices of derivatives: Spectral algorithm for solving multiterm variable-order fractional differential equations. *Bound. Value Probl.* **2023**, *2023*, 108. [CrossRef]
42. Abd El-Hady, M.; El-Gamel, M.; Emadifar, H. Analysis of RL electric circuits modeled by fractional Riccati IVP via Jacobi-Broyden Newton algorithm. *PLoS ONE* **2025**, *20*, e0316348. [CrossRef]
43. Ahmed, H.M. New generalized Jacobi polynomial Galerkin operational matrices of derivatives: An algorithm for solving boundary value problems. *Fractal Fract.* **2024**, *8*, 199. [CrossRef]
44. Youssri, Y.H.; Ismail, M.I.; Atta, A.G. Chebyshev Petrov-Galerkin procedure for the time-fractional heat equation with nonlocal conditions. *Phys. Scr.* **2023**, *99*, 015251. [CrossRef]
45. Singh, H.; Srivastava, H.M. Jacobi collocation method for the approximate solution of some fractional-order Riccati differential equations with variable coefficients. *Physica A* **2019**, *523*, 1130–1149. [CrossRef]
46. Ahmed, H.M. Highly accurate method for a singularly perturbed coupled system of convection–diffusion equations with Robin boundary conditions. *J. Nonlinear Math. Phys.* **2024**, *31*, 17. [CrossRef]
47. Abdelkawy, M.A.; Izadi, M.; Adel, W. Robust and accurate numerical framework for multi-dimensional fractional-order telegraph equations using Jacobi/Jacobi–Romanovski spectral technique. *Bound. Value Prob.* **2024**, *2024*, 131. [CrossRef]
48. Kazem, S.; Abbasbandy, S.; Kumar, S. Fractional-order Legendre functions for solving fractional-order differential equations. *Appl. Math. Model.* **2013**, *37*, 5498–5510. [CrossRef]
49. Rahimkhani, P.; Ordokhani, Y.; Babolian, E. Fractional-order Bernoulli wavelets and their applications. *Appl. Math. Model.* **2016**, *40*, 8087–8107. [CrossRef]
50. Bhrawy, A.H.; Zaky, M.A. Shifted fractional-order Jacobi orthogonal functions: Application to a system of fractional differential equations. *Appl. Math. Model.* **2016**, *40*, 832–845. [CrossRef]
51. Yin, F.; Song, J.; Wu, Y.; Zhang, L. Numerical solution of the fractional partial differential equations by the two-dimensional fractional-order Legendre functions. *Abstr. Appl. Anal.* **2013**, *2013*, 562140. [CrossRef]
52. Izadi, M.; Cattani, C. Generalized Bessel polynomial for multi-order fractional differential equations. *Symmetry* **2020**, *12*, 1260. [CrossRef]
53. Bhrawy, A.H.; Alghamdi, M.M.; Taha, T.M. A new modified generalized Laguerre operational matrix of fractional integration for solving fractional differential equations on the half line. *Adv. Differ. Equ.* **2012**, *2012*, 179. [CrossRef]
54. Shahriyar, M.R.B.; Ismail, F.; Aghabeigi, S.; Ahmadian, A.; Salahshour, S. An eigenvalue-eigenvector method for solving a system of fractional differential equations with uncertainty. *Math. Probl. Eng.* **2013**, *2013*, 579761. [CrossRef]
55. Eghbali, A.; Johansson, H.; Saramäki, T. A method for the design of Farrow-structure based variable fractional-delay FIR filters. *Signal Process.* **2013**, *93*, 1341–1348. [CrossRef]
56. Yu, C.; Teo, K.L.; Dam, H.H. Design of allpass variable fractional delay filter with signed powers-of-two coefficients. *Signal Process.* **2014**, *95*, 32–42. [CrossRef]
57. Cooper, G.R.J; Cowan, D.R. Filtering using variable order vertical derivatives. *Comput. Geosci.* **2004**, *30*, 455–459. [CrossRef]
58. Tseng, C.-C. Design of variable and adaptive fractional order FIR differentiators. *Signal Process.* **2006**, *86*, 2554–2566. [CrossRef]

59. Coimbra, C.F.M. Mechanics with variable-order differential operators. *Ann. Phys.* **2003**, *515*, 692–703. [CrossRef]
60. Szegö, G. *Orthogonal Polynomials*; American Mathematical Society: Providence, RI, USA, 1975; Volume XXIII.
61. Kamali, F.; Saeedi, H. Generalized fractional-order Jacobi functions for solving a nonlinear systems of fractional partial differential equations numerically. *Math. Methods Appl. Sci.* **2018**, *41*, 3155–3174. [CrossRef]
62. Burden, R.L.; Faires, J.D.; Burden, A.M. *Numerical Analysis*; Cengage Learning: Boston, MA, USA, 2015.
63. Jeffrey, A.; Dai, H.H. *Handbook of Mathematical Formulas and Integrals*; Elsevier: Amsterdam, The Netherlands, 2008.
64. Irandoust-Pakchin, S.; Kheiri, H.; Abdi-Mazraeh, S. Efficient computational algorithms for solving one class of fractional boundary value problems. *Comp. Math. Math. Phys.* **2013**, *53*, 920–932. [CrossRef]
65. Hassani, H.; Dahaghin, M.S.; Heydari, H. A new optimized method for solving variable-order fractional differential equations. *J. Math. Ext.* **2017**, *11*, 85–98.

Disclaimer/Publisher's Note: The statements, opinions and data contained in all publications are solely those of the individual author(s) and contributor(s) and not of MDPI and/or the editor(s). MDPI and/or the editor(s) disclaim responsibility for any injury to people or property resulting from any ideas, methods, instructions or products referred to in the content.